Dissection of Upstream Regulatory Components of the Rho1p Effector, 1,3-β-Glucan Synthase, in *Saccharomyces cerevisiae*

Mariko Sekiya-Kawasaki,*[,1] Mitsuhiro Abe,*[,1] Ayaka Saka,* Daisuke Watanabe,* Keiko Kono,* Masayo Minemura-Asakawa,* Satoru Ishihara,* Takahide Watanabe[†] and Yoshikazu Ohya*[,‡,2]

**Department of Integrated Biosciences, Graduate School of Frontier Science, University of Tokyo, Kashiwanoha, Kashiwa, Chiba 277-8562, Japan, [†]Department of Mycology, Nippon Roche Research Center, Kajiwara, Kamakura, Kanagawa 247-8530, Japan and [‡]Unit Process and Combined Circuit, PRESTO, Japan Science and Technology Corporation, Shinsenri-Higashimachi, Toyonaka, Osaka 565-0082, Japan*

Manuscript received June 24, 2002
Accepted for publication July 15, 2002

ABSTRACT

In the budding yeast *Saccharomyces cerevisiae*, one of the main structural components of the cell wall is 1,3-β-glucan produced by 1,3-β-glucan synthase (GS). Yeast GS is composed of a putative catalytic subunit encoded by *FKS1* and *FKS2* and a regulatory subunit encoded by *RHO1*. A combination of amino acid alterations in the putative catalytic domain of Fks1p was found to result in a loss of the catalytic activity. To identify upstream regulators of 1,3-β-glucan synthesis, we isolated multicopy suppressors of the GS mutation. We demonstrate that all of the multicopy suppressors obtained (*WSC1*, *WSC3*, *MTL1*, *ROM2*, *LRE1*, *ZDS1*, and *MSB1*) and the constitutively active *RHO1* mutations tested restore 1,3-β-glucan synthesis in the GS mutant. A deletion of either *ROM2* or *WSC1* leads to a significant defect of 1,3-β-glucan synthesis. Analyses of the degree of Mpk1p phosphorylation revealed that among the multicopy suppressors, *WSC1*, *ROM2*, *LRE1*, *MSB1*, and *MTL1* act positively on the Pkc1p-MAPK pathway, another signaling pathway regulated by Rho1p, while *WSC3* and *ZDS1* do not. We have also found that *MID2* acts positively on Pkc1p without affecting 1,3-β-glucan synthesis. These results suggest that distinct networks regulate the two effector proteins of Rho1p, Fks1p and Pkc1p.

THE cell wall is a fundamentally rigid structure that defines the shape of plant and fungal cells. During morphogenesis of vegetatively growing cells of the budding yeast *Saccharomyces cerevisiae*, cell wall materials are incorporated into the restricted cell surface domain active for cell wall remodeling (Cid *et al.* 1995). Therefore, it is conceivable that numerous signals representing spatial and temporal information are integrated into cell wall synthesis during the budding process. Although a number of proteins essential for establishment of cell polarity have been identified (Pruyne and Bretscher 2000a,b), little is known about how cell polarity and spatial activation of cell wall synthesis are related.

The structural components of the yeast cell wall are 1,3-β-glucan polymer with some branches of 1,6-β-linkages, chitin, and mannoproteins. Among them, 1,3-β-glucan is the main component responsible for the rigidity of yeast cells. 1,3-β-glucan synthase (GS) is composed of a putative catalytic subunit and a regulatory subunit. The putative catalytic subunit is an integral membrane protein encoded by the two closely related genes, Fks1p and Fks2p (Douglas *et al.* 1994; Inoue *et al.* 1995; Mazur *et al.* 1995). Double deletions of *FKS1* and *FKS2* are inviable (Inoue *et al.* 1995; Mazur *et al.* 1995), indicating functional redundancy between Fks1p and Fks2p. The regulatory subunit is copurified with GS and encoded by *RHO1* (Drgonová *et al.* 1996; Mazur and Baginsky 1996; Qadota *et al.* 1996). Rho1p acts as a molecular switch and specifically activates its effectors in its GTP-bound form (Cabib *et al.* 1998). Thus, Rho1p likely has the ability to monitor and to receive upstream signals that direct cell wall remodeling and cell morphogenesis.

In addition to Fks1p/Fks2p, four effector molecules of yeast Rho1p have thus far been known. Rho1p binds and activates Pkc1p, which in turn stimulates the Pkc1p-mitogen-activated protein kinase cascade (Pkc1p-Mpk1p pathway) to organize actin cytoskeleton and to maintain cell integrity (Paravicini *et al.* 1992; Nonaka *et al.* 1995; Kamada *et al.* 1996; Helliwell *et al.* 1998). Rho1p also interacts with Bni1p, a yeast homolog of formin (Kohno *et al.* 1996). Bni1p might regulate actin cytoskeleton through interaction with an actin-binding protein, profilin (Evangelista *et al.* 1997; Imamura *et al.* 1997). Rho1p also binds to Skn7p (Alberts *et al.* 1998), which is thought to function in oxidative stress response (Morgan *et al.* 1997), in transcription during G1-S phase (Bouquin *et al.* 1999), and in the two-component regulatory pathway (Brown *et al.* 1994). Furthermore, the active form of Rho1p interacts with Sec3p, a spatial landmark for polar-

[1]These authors contributed equally to this work.

[2]*Corresponding author:* Department of Integrated Biosciences, Graduate School of Frontier Science, University of Tokyo, Bldg. FSB-101, 5-1-5 Kashiwanoha, Kashiwa, Chiba 277-8562, Japan.
E-mail: ohya@k.u-tokyo.ac.jp

ized exocytosis, and Rho1p is required for the establishment and maintenance of the Sec3p localization (Guo *et al.* 2001).

Screens of components that physically and genetically interact with Rho1p have led to the identification of various Rho1p activators in yeast: Multicopy suppressor screening using a conditional *rho1* mutant identified Rom1p and Rom2p, GDP-GTP exchange factors (GEF) of Rho1p (Ozaki *et al.* 1996). Two-hybrid screening using an *RHO1* fragment identified Bem4p, which positively affects Rho1p function by a mechanism other than promotion of GDP-to-GTP exchange of Rho1p (Hirano *et al.* 1996). *WSC* family genes and the functionally related *MID2* and *MTL1* genes were genetically placed upstream of *RHO1* and the Pkc1p-mitogen-activated protein kinase (MAPK) cascade (Gray *et al.* 1997; Verna *et al.* 1997; Jacoby *et al.* 1998; Ketela *et al.* 1999; Rajavel *et al.* 1999). Both Wsc1p and Mid2p interact with Rom2p and stimulate nucleotide exchange activity toward Rho1p (Philip and Levin 2001). Although these factors have been shown to act upstream of the Pkc1p-MAPK cascade (Kamada *et al.* 1995; Verna *et al.* 1997; Martín *et al.* 2000; Philip and Levin 2001), the roles of Rho1p regulators on 1,3-β-glucan synthesis remain unknown.

In this study, we have taken a genetic approach to isolate factors involved in 1,3-β-glucan synthesis. We performed a high-copy suppressor screen using *fks1-1154 fks2*Δ, a temperature-sensitive mutant of GS (simply referred to as *fks1-1154* below). By detecting *in vivo* glucan synthesis with aniline blue, a specific fluorescent dye for 1,3-β-glucan, and by incorporating labeled glucose into cell wall 1,3-β-glucan, we showed that all the suppressors act positively on 1,3-β-glucan synthesis. In addition, we examined whether the suppressors act positively on the Pkc1p-MAPK cascade. On the basis of these results we present a model of the molecular network upstream of Fks1p and Pkc1p.

MATERIALS AND METHODS

Media, growth conditions, and genetic manipulation: Tetrad analysis and mating-type determination were performed as described previously (Kaiser *et al.* 1994). Yeast transformation was carried out using the lithium acetate method (Ito *et al.* 1983). Yeast cells were grown in rich medium (YPD) [1% Bacto yeast extract (Difco, Detroit), 2% polypeptone (Nihon Seiyaku, Tokyo), and 2% glucose (Wako Chemicals, Osaka, Japan)], or in synthetic growth medium (SD) [0.67% yeast nitrogen base (Difco) and 2% glucose] appropriately supplemented. To examine a phenotype of the cells with a reduced GS activity, we grew yeast cells in a 0.2% glucose medium [1% Bacto yeast extract, 2% polypeptone, and 0.2% glucose]. Sensitivity to echinocandin B and Calcofluor white were examined as previously (Ram *et al.* 1994; Inoue *et al.* 1995). For -Ura or -Trp selection, 0.5% casamino acid (Difco, Detroit) was added to SD. Standard procedures were used for all DNA manipulations and *Escherichia coli* transformation (Sambrook *et al.* 1989).

Strains: The yeast strains used are listed in Table 1. All the strains are isogenic derivatives of YPH499, YPH500, or YPH501. To construct YOC748 (*msb1*Δ), we replaced the 3.3-kb *Eco*RI-to-*Sph*I fragment inside the open reading frame (ORF) of *MSB1* with a DNA fragment containing the *HIS3* gene (from pJJ217). YOC2521 (*wsc3*Δ), YOC2526 (*mid2*Δ *mtl1*Δ), YOC2573 (*wsc1*Δ), YOC2576 (*rom2*Δ), YOC2579 (*lre1*Δ), and YOC2581 (*zds1*Δ) were constructed by PCR-mediated gene disruptions described previously (Sakumoto *et al.* 1999): Primers were used to amplify the *HIS3*, *LEU2*, or *TRP1* gene of *Candida glabrata* together with flanking sequences derived from the upstream and downstream regions of the corresponding genes. Details of YOC1001 (*FKS1 fks2*Δ) and YOC1087 (*fks1-1154 fks2*Δ) constructions will be described elsewhere (M. Abe, M. Minemura-Asakawa, T. Utsugi, M. Sekiya-Kawasaki, A. Hirata, H. Qadota, K. Morishita, T. Watanabe and Y. Ohya, unpublished results). Briefly, YOC1087 is a temperature-sensitive strain with the *FKS1* and *FKS2* genes deleted and a mutant allele of *fks1* (*fks1-1154*) integrated at the *ADE3* locus. YOC1001 is a wild-type control of YOC1087 with *FKS1* and *FKS2* deleted and the wild-type *FKS1* gene integrated at the *ADE3* locus.

Plasmids: The plasmids used in this study are listed in Table 2. A YEp13-based genomic library was described previously (Yoshihisa and Anraku 1989).

pYO971: The *Kpn*I-*Sac*I fragment of pRS316 was replaced with a *Kpn*I-*Nhe*I-*Sph*I-*Sac*I linker.

pYO326NS: Using a linker, *Nhe*I and *Sph*I sites were inserted adjacent to the *Sma*I site of pYO326.

pYO964 and *pYO965*: *RHO1* mutations (G19V and Q68L) were introduced by two-step PCR mutagenesis (Ho *et al.* 1989). The mutated *RHO1* open reading frames were inserted into pYO701, which consists of pRS314, the 0.2-kb *RHO1* promoter, and the 0.1-kb *RHO1* terminator (Qadota *et al.* 1994). To construct pYO964 and pYO965, we cloned the mutant *RHO1* genes into pRS316.

pYO2358: 7.8-kb *Sph*I-*Nhe*I fragment including the entire ORF of *FKS1* from pGSYE1 (Inoue *et al.* 1995) was inserted into pYO326NS.

pYO2325: A genomic fragment containing the *MTL1* ORF, plus 1 kbp upstream and 500 bp downstream, was amplified from the *S. cerevisiae* genome by high-fidelity PCR using primers that generate a *Sal*I site at the 5′-end. The PCR product was cloned into pYO326. The DNA sequence of the cloned *MTL1* gene was verified.

pYO2361: A 1.9-kb *Hpa*I-*Xho*I fragment including *MID2* (derived from the YEp13 genomic bank) was cloned into pYO326.

pYO2364: A 2.7-kb *Bgl*II-*Bgl*II fragment including *WSC1* (derived from the YEp13 genomic bank) was cloned into pYO326.

pYO2366: A 6.5-kb *Hpa*I-*Hpa*I fragment including *ROM2* (derived from the YEp13 genomic bank) was cloned into pYO326.

pYO2368: A 2.5-kb *Eco*RV-*Eco*RV fragment including *LRE1* (derived from the YEp13 genomic bank) was cloned into pYO326.

pYO2369: A 3.4-kb *Eco*RI-*Sph*I fragment including *WSC3* ORF, plus 0.9 kb upstream and 0.8 kb downstream (derived from the YEp13 genomic bank), were cloned into pYO326. The *Sph*I site is on the YEp13 vector.

pYO2370: A 3.7-kb *Eco*RI-*Cla*I fragment including *ZDS1* ORF, plus 0.3 kb upstream and 0.6 kb downstream (derived from the YEp13 genomic bank), were cloned into pYO326. The *Cla*I site is on the YEp13 vector.

pYO2371: A 5.5-kb *Sal*I-*Bam*HI fragment including *MSB1* (derived from the YEp13 genomic bank) was cloned into pYO326.

TABLE 1

Yeast strains

Strain	Genotype	Reference
YPH499	*MAT***a** *ade2 his3 leu2 lys2 trp1 ura3*	Sikorski and Hieter (1989)
YPH500	*MAT***a** *ade2 his3 leu2 lys2 trp1 ura3*	Sikorski and Hieter (1989)
YPH501	*MAT***a**/*MAT*α *ade2/ade2 his3/his3 leu2/leu2 lys2/lys2 trp1/trp1 ura3/ura3*	Sikorski and Hieter (1989)
YOC748	*MAT*α *ade2 his3 leu2 lys2 trp1 ura3 msb1*Δ*::HIS3*	This study
YOC752	*MAT*α *ade2 his3 leu2 lys2 trp1 ura3 rho1*Δ*::HIS3 ade3::rho1-2::LEU2*	Qadota *et al.*(1996)
YOC1001	*MAT***a** *ade2 his3 leu2 lys2 trp1 ura3 fks1*Δ*::HIS3 fks2*Δ*::LYS2 ade3::FKS1::TRP1*	This study
YOC1087	*MAT***a** *ade2 his3 leu2 lys2 trp1 ura3 fks1*Δ*::HIS3 fks2*Δ*::LYS2 ade3::fks1-1154::TRP1*	This study
YOC2521	*MAT***a** *ade2 his3 leu2 lys2 trp1 ura3 wsc3*Δ*::cgHIS3*[a]	This study
YOC2526	*MAT***a** *ade2 his3 leu2 lys2 trp1 ura3 mid2*Δ*::cgLEU2 mtl1*Δ*::cgHIS3*[a]	This study
YOC2573	*MAT***a** *ade2 his3 leu2 lys2 trp1 ura3 wsc1*Δ*::cgLEU2*[a]	This study
YOC2576	*MAT*α *ade2 his3 leu2 lys2 trp1 ura3 rom2*Δ*::cgTRP1*[a]	This study
YOC2579	*MAT***a** *ade2 his3 leu2 lys2 trp1 ura3 lre1*Δ*::cgTRP1*[a]	This study
YOC2581	*MAT***a** *ade2 his3 leu2 lys2 trp1 ura3 zds1*Δ*::cgHIS3*[a]	This study

[a] *cgHIS3*, *cgLEU2*, and *cgTRP1* indicate *C. glabrata HIS3*, *LEU2*, and *TRP1* genes, respectively.

Multicopy suppressor screening: YOC1087 (*fks1-1154*) was transformed with a 2μ-based genomic library with a 5- to ~10-kb insert for each clone. Out of ~40,000 colonies, transformants growing at 37° were isolated. Then we rescued the plasmids responsible for suppression and retransformed the parental strain with them to recheck suppression. The inserts were directly sequenced and the clones containing *FKS1* (6 clones) and *FKS2* (15 clones) were excluded from further investigation. We carried out subcloning using standard techniques to determine which ORFs are responsible for suppression. Finally, we identified six genes (*WSC1*, *WSC3*, *ROM2*, *LRE1*, *ZDS1*, and *MSB1*) that are responsible for suppression when expressed on a multicopy vector. We independently isolated 3 *WSC1* clones, 8 *WSC3* clones, 2 *ROM2* clones, 2 *LRE1* clones, 4 *ZDS1* clones, and 3 *MSB1* clones.

Morphological observations: For staining of yeast cells with aniline blue, early log-phase cells (~1×10^7 cells) were harvested by low-speed centrifugation (2000 rpm, 3 min). The cells were washed twice with PBS and mildly sonicated for 10–20 sec. The washed and sonicated cells were incubated with 0.05% aniline blue (Wako) for 5 min and then observed under the fluorescence microscope using the Olympus U-MNV DM455 filter set (excitation wavelength, 400–410 nm; emission wavelength, 455 nm). Procedures for immunofluorescence microscopy were as described previously (Pringle *et al.* 1989). For Fks1p staining, a mouse monoclonal antibody to Fks1p (T2B8; Inoue *et al.* 1995) was selected as a primary antibody and a FITC-conjugated goat anti-mouse antibody was used as a secondary antibody at a 1:50 dilution. Cells were viewed on an Olympus BX-FLA microscope (Olympus, Tokyo). Images were captured using a CCD camera (Olympus MicroMax/OL) and Metamorph Imaging software (Universal Imaging,

TABLE 2

Plasmids used in this study

Name	Parent plasmid	Markers	Reference
pJJ217	pUC18	*HIS3*	Jones and Prakash (1990)
pJJ283	pUC18	*LEU2*	Jones and Prakash (1990)
pRS316		*URA3*, *CEN*	Sikorski and Hieter (1989)
pYO971	pRS316	*URA3*, *CEN*	This study
pYO326	pRS306	*URA3*, 2μ origin	Qadota *et al.* (1994)
pYO326NS	pYO326	*URA3*, 2μ origin	This study
pYO701	pRS314	*TRP1*, *RHO1* promoter, *RHO1* terminator, *CEN*	Qadota *et al.* (1994)
pYO962 [YCpL-*RHO1*(Q68L)]	pRS315	*LEU2*, *RHO1(Q68L)*, *CEN*	This study
pYO964 [YCpU-*RHO1*(G19V)]	pRS316	*URA3*, *RHO1(G19V)*, *CEN*	This study
pYO965 [YCpU-*RHO1*(Q68L)]	pRS316	*URA3*, *RHO1(Q68L)*, *CEN*	This study
pYO1835 (YEpU-*RHO1*)	pYO326	*URA3*, *RHO1*, 2μ origin	This study
pYO2325 (YEpU-*MTL1*)	pYO326	*URA3*, *MTL1*, 2μ origin	This study
pYO2358 (YEpU-*FKS1*)	pYO326	*URA3*, *FKS1*, 2μ origin	This study
pYO2361 (YEpU-*MID2*)	pYO326	*URA3*, *MID2*, 2μ origin	This study
pYO2364 (YEpU-*WSC1*)	pYO326	*URA3*, *WSC1*, 2μ origin	This study
pYO2366 (YEpU-*ROM2*)	pYO326	*URA3*, *ROM2*, 2μ origin	This study
pYO2368 (YEpU-*LRE1*)	pYO326	*URA3*, *LRE1*, 2μ origin	This study
pYO2369 (YEpU-*WSC3*)	pYO326	*URA3*, *WSC3*, 2μ origin	This study
pYO2370 (YEpU-*ZDS1*)	pYO326	*URA3*, *ZDS1*, 2μ origin	This study
pYO2371 (YEpU-*MSB1*)	pYO326	*URA3*, *MSB1*, 2μ origin	This study

West Chester, PA). All the images presented were processed using Adobe PhotoShop software.

Incorporation of [^{14}C]glucose into 1,3-β-glucan: Labeling of 1,3-β-glucan was carried out as described previously (Hong *et al.* 1994) with some modifications. Cells were grown to early log phase at 25° and shifted to appropriate temperature for 2 hr. Cells were diluted to OD_{600} of 0.5 with 1 ml of low-glucose medium [1% Bacto yeast extract, 2% polypeptone, and 0.5% glucose] or 0.67% yeast nitrogen base and 0.5% glucose containing 10 μCi of [^{14}C]glucose and labeled for 2 hr. Labeled cells were harvested at 4° and extracted with 1 N NaOH at 75° for 1 hr. The insoluble fraction was collected and washed two times with distilled water (DW). The insoluble pellet was resuspended in 300 μl of 10 mM Tris/HCl, pH 7.5, containing 5 mg/ml zymolyase 100T (Seikagaku) and incubated at 37° for 20 hr. After digestion, the zymolyase-resistant material was removed by centrifugation (15,000 × *g* for 20 min). The supernatant was filtered through a microcon-10 membrane (Amicon Bioseparations, Beverly, MA). The flow-through fraction was dried with a vacuum evaporator, resuspended in 20 μl of DW, and applied to Unifilter-GF/C (Packard Instrument, Meriden, CT). The difference in the incorporation rate for the strain was normalized by ΔOD_{600} that was determined before and after the labeling period.

Quantitative 1,3-β-glucan measurements: Amount of 1,3-β-glucan per cell was measured using aniline blue as described previously (Watanabe *et al.* 2001) with some modifications. Cells were grown to early log phase and 2.5×10^6 cells were harvested. The cells were washed twice with TE and resuspended in 500 μl TE. To the cells 6 N NaOH was added to a final concentration of 1 N, floated in a water bath at 80° for 30 min followed by addition of 2.1 ml of AB mix [0.03% aniline blue (Wako), 0.18 N HCl, and 0.49 M glycine/NaOH, pH 9.5]. The tube was vortexed briefly and then incubated at 50° for 30 min and an additional 30 min at room temperature to allow reaction with the fluorochrome and decolorization of the aniline blue. Fluorescence of 1,3-β-glucan was quantified using a spectrofluorophotometer (RF-5300PC, Shimadzu, Kyoto, Japan). Excitation wavelength was 400 nm/slit, width 3 nm, and emission wavelength was 460 nm/slit, width 3 nm.

Assay of *in vitro* GS activity: The membrane fraction was prepared as described previously (Abe *et al.* 2001). In brief, log-phase cultures were resuspended in 1 mM EDTA and 500 mM NaCl containing 1 mM phenylmethylsulfonyl fluoride and lysed with glass beads. The crude lysate was centrifuged at 1500 × *g* for 5 min so that cell debris and unbroken cells are separated. After a centrifugation at 100,000 × *g* for 30 min, the pellet was suspended in a buffer containing 50 mM Tris-HCl (pH 7.5), 1 mM EDTA, and 33% glycerol, and the suspension was used as the membrane fraction. GS activity was measured according to the procedure described previously (Inoue *et al.* 1995). As described (Inoue *et al.* 1995), the assay buffer (composition of the assay buffer) contains an excess amount of GTPγS.

Immunoblot analysis of Mpk1p: Cells were grown to the log phase at 25° in SD-Ura medium and shifted to 39° for 2 hr. The cell extracts were prepared as described (Martín *et al.* 2000). Protein samples (50 μg) were loaded on SDS-polyacrylamide gels, transferred to PVDF membranes (Amersham Bioscience, catalog no. RPN2020F), and blotted with either an anti-phospho-p44/42 MAPK (Thr^{202}/Tyr^{204}) antibody (catalog no. 9101, New England Biolabs, Beverly, MA) or an anti-MAPK antibody (catalog no. sc-6802, Santa Cruz Biotechnology). After reacting with ECL-Plus (Amersham Bioscience), the amount of each protein was quantified with LAS-1000plus (Fuji Photo Film).

RESULTS

1,3-β-Glucan synthesis is defective in *fks1-1154 fks2*Δ cells: A temperature-sensitive mutant, *fks1-1154* (K877N, A899S, Q977P) *fks2*Δ (referred to as *fks1-1154* below), was isolated in a genetic study of GS function in *S. cerevisiae* (M. Abe, M. Minemura-Asakawa, T. Utsugi, M. Sekiya-Kawasaki, A. Hirata, H. Qadota, K. Morishita, T. Watanabe and Y. Ohya, unpublished results). The *fks1-1154* mutant was able to grow at 25°, but failed to grow >35°. The mutation sites of *fks1-1154* are located within the hydrophilic sequences representing the putative catalytic domain (Kelly *et al.* 1996). As expected, the membrane fraction of *fks1-1154* cells was virtually devoid of GS activity (Figure 1A). A kinetic analysis of GS activity of the membrane fraction revealed that the *fks1-1154* mutant has decreased V_{max} values, which are one-fifth that of wild-type cells at 25° and one-seventh that of wild-type cells at 37°, while the K_m value was not significantly changed (data not shown). Since GS activities of membrane fraction were measured in the presence of GTPγS, Rho1p in the *in vitro* reaction was assumed to be in its active state while Rho1p *in vivo* is supposed to be not fully activated. Next, to examine the *in vivo* 1,3-β-glucan synthesis, we measured incorporation of [^{14}C]glucose into the 1,3-β-glucan. Incorporation of glucose at 37° was also severely reduced in the *fks1-1154* mutant (Figure 1B). Thus, in both physiological and Rho1p-activated conditions, GS activities of the *fks1-1154* mutant are dramatically reduced at the restrictive temperature, suggesting that the activity of Fks1-1154p is below the required minimum value for viability at 37°.

We next examined the growth phenotypes of the *fks1-1154* cells. We found that the *fks1-1154* cells are hypersensitive to a specific inhibitor of 1,3-β-glucan synthase, echinocandin B (Hector 1993; Debono and Gordee 1994), and to a chitin-binding reagent, Calcofluor white (Roncero and Durán 1985; Ram *et al.* 1994). In addition, the *fks1-1154* cells failed to grow in a low-glucose medium, in which synthesis of 1,3-β-glucan is limited. These results are consistent with the idea that GS in *fks1-1154* cells is devoid of catalytic activity of GS.

Next, to monitor *in vivo* 1,3-β-glucan synthesis in *fks1-1154* cells, we stained mutant cells with aniline blue, a fluorescent dye that preferentially interacts with 1,3-β-glucan. It is known that fluorescent intensity derived from aniline blue increases with the amount of associated 1,3-β-glucan (Evans and Hoyne 1984; Shedletzky *et al.* 1997). The wild-type cells exhibited uniform staining of the cell wall on the entire cell surface, but most of the *fks1-1154* cells appear to lose staining signal specifically in the bud at the restrictive temperature (Figure 1, C and D). A slight defect of *fks1-1154* was observed at the permissive temperature (Figure 1D, 25°, solid bars). On the basis of these facts, we suggest that the *fks1-1154* strain is severely defective in the synthesis of

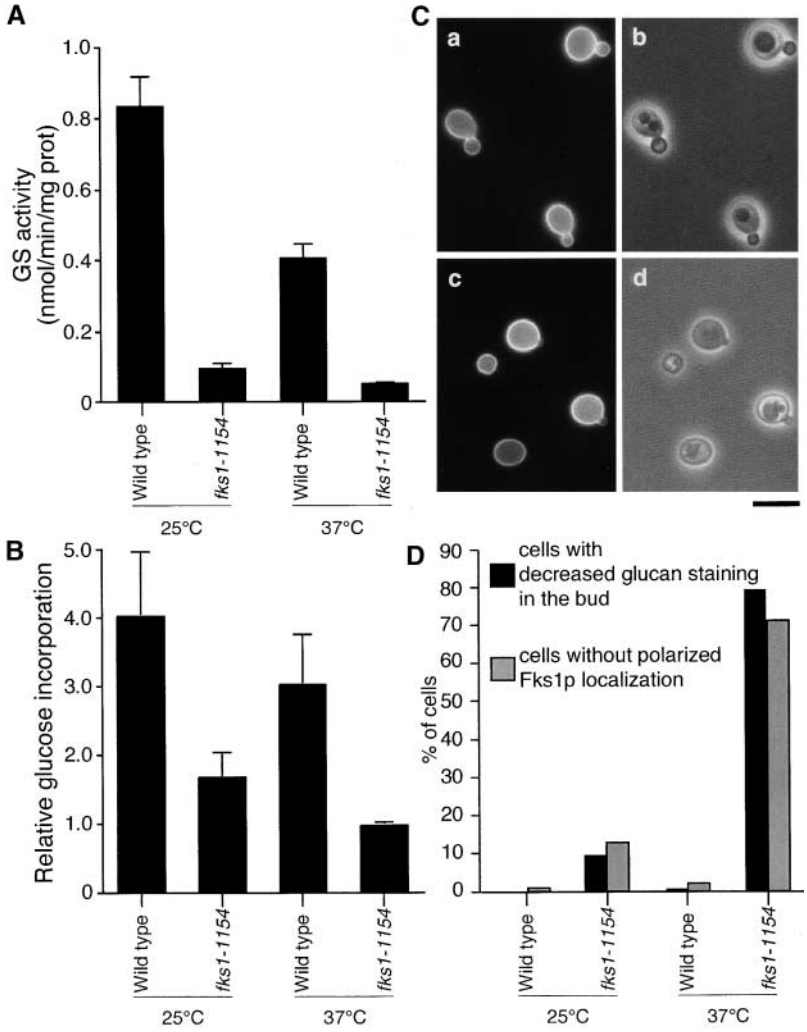

FIGURE 1.—Defective *in vivo* glucan synthesis of *fks1-1154* cells. (A) *In vitro* glucan synthase activity of the membrane fraction of *fks1-1154*. *fks1-1154* cells were incubated at 25° or shifted to 37° for 2 hr and then assayed for GS activity. The data represent the means and standard deviations of at least four experiments. Strains used: YOC1001 (wild type) and YOC1087 (*fks1-1154*). (B) Incorporation of glucose into 1,3-β-glucan of *fks1-1154*. Cells were incubated at 25° or shifted to 37° for 2 hr, labeled with [^{14}C]glucose for 2 hr, and measured for incorporation of glucose into 1,3-β-glucan. The data represent the means and standard deviations of at least three experiments. Strains used: YOC1001 (wild type) and YOC1087 (*fks1-1154*). (C) AB staining of yeast cells. Cells were shifted from 25° to 37°, cultured for 4 hr, and then stained with aniline blue. (a and b) YOC1001 (wild type); (c and d) YOC1087 (*fks1-1154*). (a and c) Glucan staining using aniline blue; (b and d) phase-contrast images. Bar, 10 μm. (D) Defective localization of Fks1p in *fks1-1154* cells. The same cells as in C were processed for observation of Fks1p localization and aniline blue staining. Cells with a small bud or tiny projections were observed. The fractions of the cells without polarized Fks1p localization (shaded bars) and those with decreased glucan staining in the bud (solid bars) were determined ($n > 200$). Strains used: YOC1001 (wild type) and YOC1087 (*fks1-1154*).

new 1,3-β-glucan into the bud. We stained other cell wall components, chitin and mannan in the *fks1-1154* cells, using Calcofluor white and FITC-Con A, respectively. Staining patterns were indistinguishable from those of the wild-type cells, suggesting that *fks1-1154* has a specific defect in 1,3-β-glucan synthesis.

Growing wild-type cells display a polarized distribution of Fks1p (QADOTA *et al.* 1996). By way of comparison, we examined the localization of Fks1p in *fks1-1154* cells and found that Fks1-1154p is delocalized slightly even at the permissive temperature and severely at the restrictive temperature (Figure 1D). Delocalization of Fks1-1154p in the *fks1-1154 fks2*Δ background was restored by introduction of *FKS2*, implying that the delocalization of Fks1-1154p in the *fks1-1154 fks2*Δ strain is due to a secondary effect of largely compromised 1,3-β-glucan synthesis.

Isolation of multicopy suppressors of *fks1-1154*: To identify genes that regulate 1,3-β-glucan synthesis, we performed a multicopy suppressor screen using the *fks1-1154* strain. We finally identified *WSC1*, *WSC3*, *ROM2*, *LRE1*, *ZDS1*, and *MSB1* as multicopy suppressors (for details of the screening, see MATERIALS AND METHODS). Since all suppressor genes were isolated as independent clones more than once, the screening was judged to be nearly saturated. Suppression of the temperature-sensitive growth defect of *fks1-1154* by several genes is shown in Figure 2. All genes isolated in the screening effectively suppressed the growth defect of the *fks1-1154* mutant at 34° (Figure 2A). We also found that constitutively active *RHO1* alleles [*RHO1* (G19V) and *RHO1* (Q68L)] expressed on a centromere plasmid were able to suppress the *fks1-1154* mutation (Figure 2A). Figure 2B shows the suppression ability at various temperatures (33°–37°): Robust growth was observed in *fks1-1154* cells transformed with multiple copies of *WSC1*, *ROM2*, *ZDS1*, or with a single copy of *RHO1* (G19V) or *RHO1* (Q68L). We also examined suppression of the low-glucose sensitive growth defect of *fks1-1154* by these suppressors. All multicopy suppressors suppress the low-glucose sensitive growth defect as well as the temperature-sensitive growth defect of *fks1-1154*. In addition, the multicopy suppressors did not suppress the synthetic lethality of *fks1*Δ *fks2*Δ double mutants (data not shown), indicat-

ing that the suppression of the growth defect is dependent on Fks1-1154p.

Wsc1p and Wsc3p are proposed to be transmembrane proteins localized on the plasma membrane and are putative upstream regulators of Pkc1p (Gray *et al.* 1997; Verna *et al.* 1997; Jacoby *et al.* 1998; Lodder *et al.* 1999). Since Mid2p and Mtl1p were shown to be functionally related to Wsc1p (Ketela *et al.* 1999; Rajavel *et al.* 1999), we asked whether overexpression of *MID2* or *MTL1* suppresses the *fks1-1154* mutation. We found that *MTL1*, but not *MID2*, weakly suppressed the growth defect of the *fks1-1154* mutant (Figure 2).

Rom2p is a GEF of Rho1p. Ozaki *et al.* (1996) reported that the phenotypes of a *rom2*Δ strain include cell lysis and the terminal phenotypes are similar to those of a *rho1* and a *pkc1* mutant, implying that Rom2p acts upstream of Rho1p and Pkc1p. Since Wsc1p, Wsc3p, Mtl1p, and Rom2p are known as putative upstream regulators of Pkc1p, one possible suppression mechanism is through Pkc1p activation. Therefore, we investigated whether stimulation of the Pkc1p-MAPK cascade rescues the defect of *fks1-1154*. We transformed *fks1-1154* cells with multiple copies of *PKC1*, an activated *PKC1* (R398P) allele (Nonaka *et al.* 1995), *BCK1* (a MAPKKK homolog), an activated *BCK1* (*BCK1-20*) allele (Lee and Levin 1992), or *MPK1* (a MAPK homolog). None of them had any effect on temperature-sensitive growth of *fks1-1154*. With the use of a specific antibody we confirmed that *PKC1* overexpression indeed increased Mpk1p phosphorylation in *fks1-1154* cells (data not shown). These results suggest that suppression of the *fks1-1154* mutation is not through Pkc1p activation. Besides the genes known to interact with Rho1p physically or genetically, three multicopy suppressors (*LRE1*, *ZDS1*, and *MSB1*) were isolated. *LRE1* was previously identified as the gene responsible for conferring resistance to laminarinase, an enzyme that specifically degrades 1,3-β-glucan (Lai *et al.* 1997). *ZDS1* was identified in numerous screens, including those designed to enhance replication origin function (Yu *et al.* 1996), to increase transcriptional silencing (Roy and Runge 1999), and to enhance the defect of *CDC42* (Bi and Pringle 1996). *MSB1* was isolated in a screen for multicopy suppressors of the *cdc24-4* mutation and was later shown to suppress a *cdc42* mutant defective in polarity establishment and cellular morphogenesis (Bender and Pringle 1989), although its function and relationship to Cdc24p and Cdc42p remain unsolved.

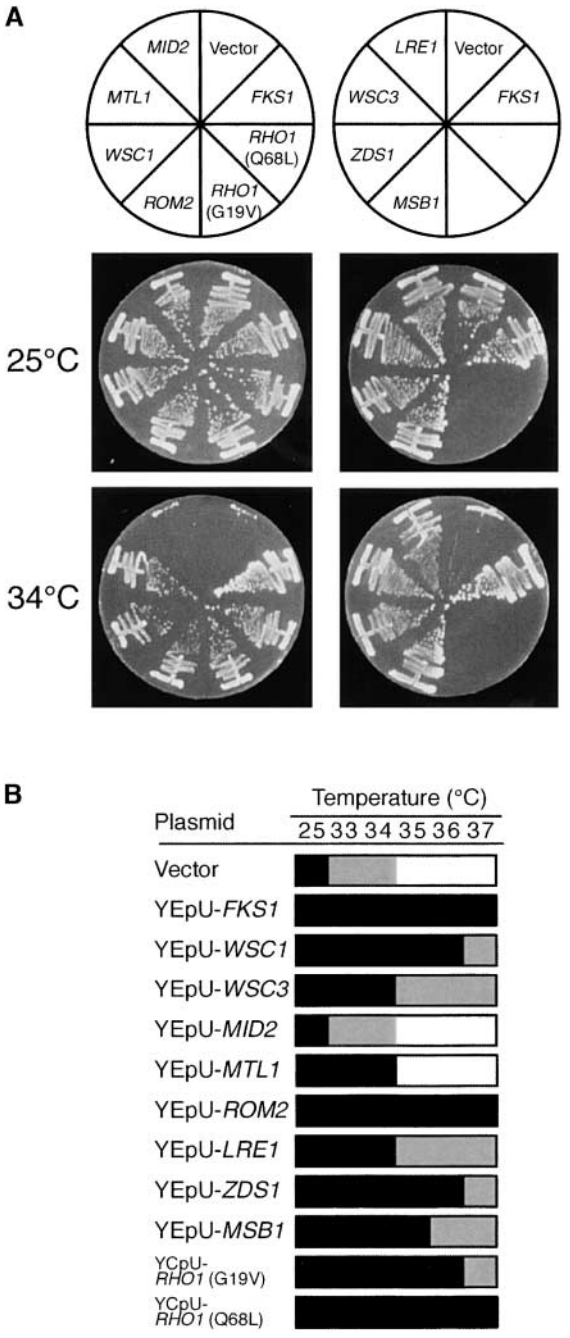

Defects of *in vivo* 1,3-β-glucan synthesis in *fks1-1154* are rescued by multicopy suppressor genes: Two possible mechanisms of multicopy suppression of the GS mutant are restoration of defective 1,3-β-glucan synthesis and reparation of compromised cell wall structure. To distinguish these two possibilities, we tested whether high dosages of the suppressors restore the defective *in vivo* glucan synthesis in *fks1-1154* cells. Using fluores-

Figure 2.—Growth of *fks1-1154* cells transformed with multicopy suppressors. (A) Growth of transformants in YPD. YOC1087 (*fks1-1154*) was transformed with either a 2μ plasmid [a control vector (pYO326), YEpU-*FKS1*, YEpU-*WSC1*, YEpU-*WSC3*, YEpU-*MID2*, YEpU-*MTL1*, YEpU-*ROM2*, YEpU-*LRE1*, YEpU-*ZDS1*, or YEpU-*MSB1*] or centromere-based plasmids [YCpU-*RHO1* (G19V) and YCpU-*RHO1* (Q68L)], streaked onto YPD plates, and incubated for 4 days at 25° (top) or 34° (bottom). (B) Growth of the transformants at various temperatures. Growth in YPD of each of the transformants used in A was scored at several temperatures. Solid, shaded, and open regions indicate growth equivalent to wild-type cells, slower growth, and no growth, respectively.

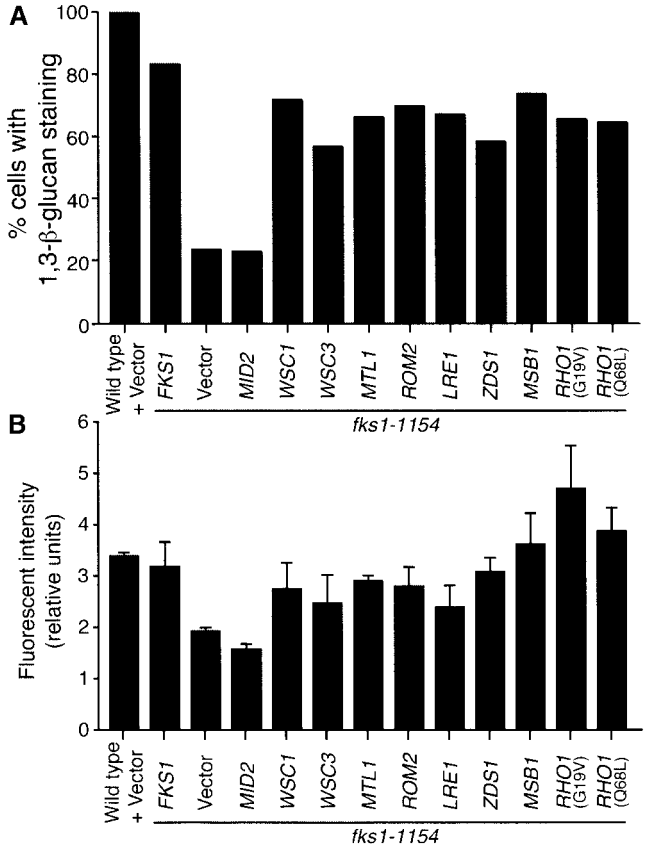

FIGURE 3.—Rescue of glucan synthesis of *fks1-1154* by the suppressors of the *fks1-1154* mutation. (A) Fractions of cells with 1,3-β-glucan staining in the bud. For aniline blue staining, cells were precultured in SD-Ura, cultured in YPD at 25° for 5 hr, and then shifted to 35° for 4 hr. Cells with a small bud or a tiny projection were observed. The transformants described in Figure 2 and a wild-type strain (YOC1001) with a control vector (pYO326) were tested. The fractions of cells with normal staining at the bud were determined ($n > 200$). (B) Quantification of the total amount of 1,3-β-glucan in *fks1-1154* cells transformed with each of the multicopy suppressor genes. Cells were cultured in SD-Ura at 25°, and the 1,3-β-glucan level per cell was measured according to MATERIALS AND METHODS and expressed as relative fluorescence intensity. Each datum represents the means and SD of at least three experiments.

cent microscopic analyses with aniline blue staining, we examined populations of cells with decreased 1,3-β-glucan staining in the bud (Figure 3A). Four hours after a shift to 35° of *fks1-1154* cells with vector alone, >70% exhibited a loss of glucan staining in the bud. In contrast, overexpression of *WSC1*, *WSC3*, *MTL1*, *ROM2*, *LRE1*, *MSB1*, *ZDS1*, and activated forms of *RHO1* significantly recovered defective glucan staining in *fks1-1154* cells (Figure 3A).

In addition to the microscopic observations, we measured incorporation of [^{14}C]glucose into 1,3-β-glucan in *fks1-1154* cells transformed with multicopy suppressor genes (Table 3). Measurements of 1,3-β-glucan revealed that *fks1-1154* cells with vector alone incubated at 34° possessed less 1,3-β-glucan compared to wild-type cells. We found that expression of all the suppressors increased the incorporation into glucan in *fks1-1154* cells. As expected from the result presented in Figure 2, overexpression of *MID2* had little effect on glucan synthesis in *fks1-1154* cells. Of the suppressors, *RHO1* (G19V) and *RHO1* (Q68L) had a relatively strong effect on recovery of glucan. Introduction of multiple copies of *WSC1*, *WSC3*, *MTL1*, *ROM2*, *LRE1*, *ZDS1*, or *MSB1* resulted in a significant increase in 1,3-β-glucan, but the level was lower than that in wild-type cells. These multicopy suppressors also rescued the reduced incorporation of [^{14}C]glucose in *fks1-1154* cells incubated at 25° in the same way (data not shown). We also quantified the total amount of 1,3-β-glucan in *fks1-1154* cells with multicopy suppressors using aniline blue (Figure 3B). Consistently, overexpression of all the suppressors increased the amount of glucan in *fks1-1154* cells while overexpression of *MID2* had little effect on glucan synthesis in *fks1-1154* cells. Together with these results (Figure 3 and Table 3), we concluded that all the suppressors have a facilitative effect on *in vivo* 1,3-β-glucan synthesis. GS activity in *fks1-1154* cells in the presence of the suppressors seems to be above the required minimum value for viability.

To examine whether these suppressors act on GS through Rho1p activation, we determined whether suppressors facilitate GS activity in cells that already have the active form of Rho1p. If a suppressor activates GS by converting Rho1p to the active form, no additional effect on GS activity will be observed. In contrast, if the suppressor activates GS in some other way, an additional effect will be seen. First, as a control experiment, we measured glucose incorporation into 1,3-β-glucan in cells expressing both the active forms of Rho1p and Rom2p. No additive effect was observed with *ROM2*

TABLE 3

Glucose incorporation into 1,3-β-glucan in *fks1-1154* cells with the multicopy suppressor genes at 34°

Strain (plasmid)	Relative incorporation into 1,3-β-glucan
fks1-1154 (pYO326)	1.00 ± 0.02
fks1-1154 (YEpU-*MID2*)	1.11 ± 0.11
fks1-1154 (YEpU-*WSC1*)	1.36 ± 0.23
fks1-1154 (YEpU-*WSC3*)	1.70 ± 0.45
fks1-1154 (YEpU-*MTL1*)	1.69 ± 0.47
fks1-1154 (YEpU-*ROM2*)	1.44 ± 0.26
fks1-1154 (YEpU-*LRE1*)	1.47 ± 0.52
fks1-1154 (YEpU-*ZDS1*)	1.51 ± 0.06
fks1-1154 (YEpU-*MSB1*)	1.56 ± 0.14
fks1-1154 [YCpL-*RHO1*(Q68L)]	2.67 ± 0.43
fks1-1154 [YCpL-*RHO1*(G19V)]	1.85 ± 0.26
FKS1 (pYO326)	3.06 ± 0.69

Each datum represents the means and SD of at least three experiments.

TABLE 4

Effect of suppressors and the active form of *RHO1* on the glucan synthesis in *fks1-1154* cells at 34°

Plasmid in *fks1-1154* cells	Relative incorporation into 1,3-β-glucan
pYO326 and YCpL-*RHO1*(Q68L)	1.00 ± 0.01
YEpU-*ROM2* and YCpL-*RHO1*(Q68L)	1.10 ± 0.07
YEpU-*WSC3* and YCpL-*RHO1*(Q68L)	1.11 ± 0.12
YEpU-*MTL1* and YCpL-*RHO1*(Q68L)	1.10 ± 0.13
YEpU-*LRE1* and YCpL-*RHO1*(Q68L)	1.04 ± 0.02
YEpU-*ZDS1* and YCpL-*RHO1*(Q68L)	1.11 ± 0.22
YEpU-*MSB1* and YCpL-*RHO1*(Q68L)	1.51 ± 0.16

The data represent the means and standard deviations of at least six experiments.

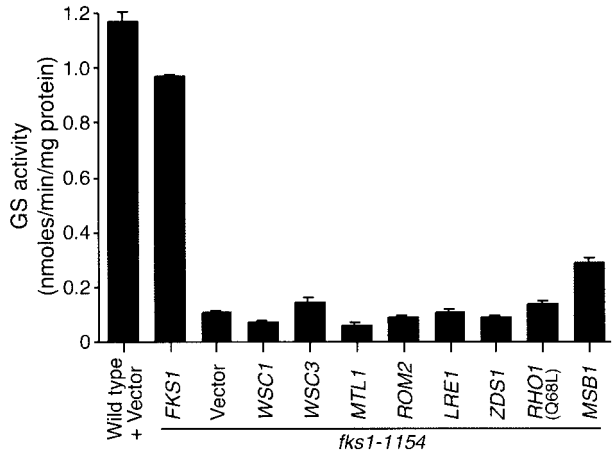

FIGURE 4.—*In vitro* glucan synthase activity assayed with the membrane fraction of *fks1-1154* transformed with a suppressor. *fks1-1154* cells transformed with one of the suppressors were shifted from 25° to 34° for 2 hr and then assayed for GS activity. The transformants described in Figure 2 and a wild-type strain (YOC1001) with a control vector (pYO326) were tested.

(Table 4), which is consistent with the previous report that Rom2p is a GEF (OZAKI *et al.* 1996), and Rom2p is required for Rho1p activation (BICKLE *et al.* 1998). Next, measurement of glucose incorporation with the active form of Rho1p and other suppressors revealed that no additive effect was observed with *WSC3*, *MTL1*, *LRE1*, or *ZDS1* (Table 4). These results suggest that Rom2p, Wsc3p, Mtl1p, Lre1p, and Zds1p act positively on GS through activation of Rho1p. On the other hand, an additive effect was observed by expressing *MSB1* (Table 4), suggesting that Msb1p acts positively on GS by mechanism(s) not involving Rho1p activation. The additive effect was phenotypically verified on the suppression of the low-glucose sensitive growth defect. Expression of both active forms of Rho1p and Msb1p caused additional suppression in the low-glucose medium, while no additive effect was observed with other multicopy suppressors. Fluorescent measurements using aniline blue also confirmed that the additive effect was observed by expressing *MSB1* and the active form of Rho1p in *fks1-1154* cells.

We also investigated how Msb1p activates GS using the membrane fractions. We measured the *in vitro* GS activity of the membrane fraction from the *fks1-1154* cells overexpressing Msb1p shifted from 25° to 34° and cultured for 2 hr. Since *in vitro* GS activity was assayed in the presence of an excess amount of GTPγS, a nonhydrolyzable analog of GTP (INOUE *et al.* 1995), virtually all Rho1p is assumed to be in its active state. If *MSB1* activates GS in some way other than Rho1p activation, an additional effect on GS activity will be seen in the presence of GTPγS. We found that *MSB1* slightly increased *in vitro* GS activity of *fks-1154* (Figure 4), supporting the idea that *in vitro* GS activity increases by a mechanism other than shifting the equilibrium of Rho1p to the GTP-bound state (see DISCUSSION). In contrast, the activities in the presence of a constitutive active *RHO1* allele and the rest of the multicopy suppressors were as low as the vector alone in the presence of GTPγS (Figure 4). These multicopy suppressors did not increase the reduced activity in *fks1-1154* cells incubated at 25° (data not shown).

Analyses of deletion strains of the multicopy suppressor genes: We constructed deletion mutants of the multicopy suppressor genes (*wsc1*Δ, *wsc3*Δ, *mid2*Δ *mtl1*Δ, *rom2*Δ, *lre1*Δ, *zds1*Δ, and *msb1*Δ) to examine their growth and *in vivo* 1,3-β-glucan synthesis. We also examined the phenotypes of a *mid2*Δ *mtl1*Δ strain because it was reported that *mid2*Δ and *mtl1*Δ showed a synthetic growth defect (KETELA *et al.* 1999; RAJAVEL *et al.* 1999). We found that among the deletion strains, *wsc1*Δ and *rom2*Δ had a significant defect in synthesis of 1,3-β-glucan at the bud (Figure 5A). These defects were more severe at the restrictive temperature than at the permissive temperature (Figure 5B). The other deletion mutants showed no detectable defects when incubated either at 30° or at 37° for 2 hr probably due to the presence of their functional redundant genes. Measurement of glucose incorporation into 1,3-β-glucan revealed that the cellular glucan synthesis in *wsc1*Δ and *rom2*Δ cells, but not those in suppressor deletion mutant cells, significantly decreased compared to that in wild-type cells (Figure 6A). The glucose incorporation did not decrease in either *mid2*Δ or *mtl1*Δ cells (data not shown). Quantitative analyses using aniline blue revealed that the amounts of 1,3-β-glucan in *wsc1*Δ and *rom2*Δ cells were reduced while other suppressor deletion mutant cells were not. We also observed that *wsc1*Δ and *rom2*Δ cells exhibited slow growth in the low-glucose medium.

Although comparison with wild-type cells showed that Fks1p is partially delocalized in *wsc1*Δ and *rom2*Δ mutant cells, most cells with defective glucan synthesis retained Fks1p at the bud at both 25° and 37° (Figure 5B). The results suggest that the defect of glucan synthesis is not

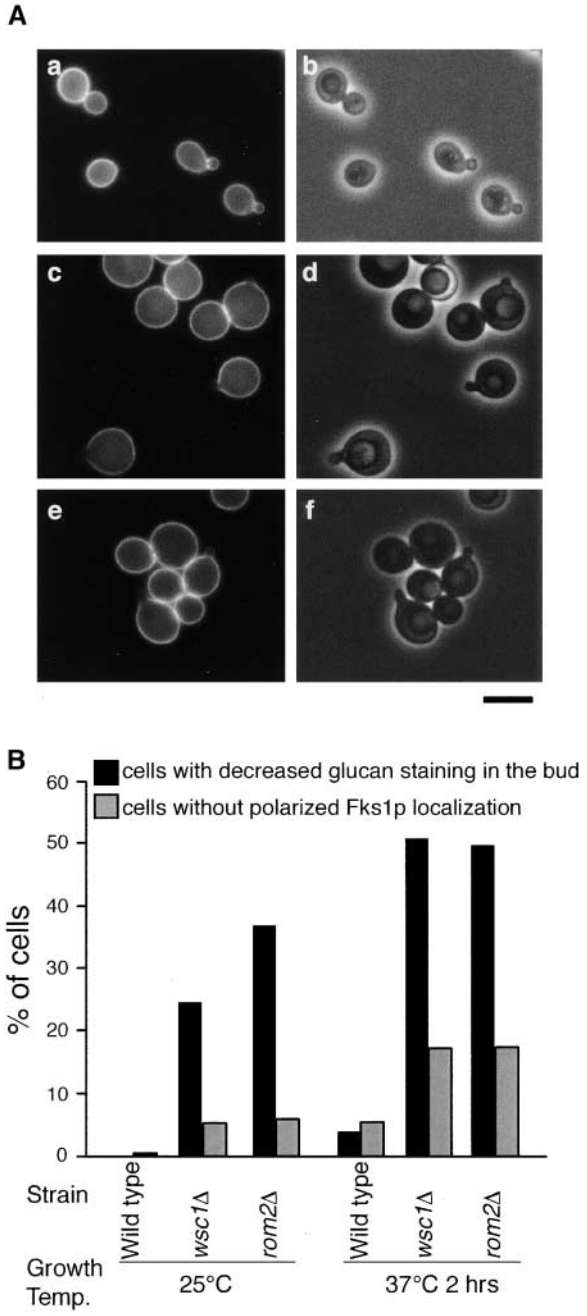

FIGURE 5.—Defects of *in vivo* glucan synthesis in *wsc1*Δ and *rom2*Δ cells. (A) *In vivo* glucan synthesis of *wsc1*Δ and *rom2*Δ cells. Cells were shifted from 25° to 37°, cultured for 2 hr, and then stained with aniline blue. (a and b) YPH499 (wild type); (c and d) YOC2573 (*wsc1*Δ); (e and f) YOC2576 (*rom2*Δ). (a, c, and e) Glucan staining with aniline blue; (b, d, and f) phase-contrast images. Bar, 10 μm. (B) Localization of Fks1p in *wsc1*Δ, *rom2*Δ cells. Cells were cultured and observed as described in Figure 1, C and D. Strains used: YPH499 (wild type), YOC2573 (*wsc1*Δ), and YOC2578 (*rom2*Δ).

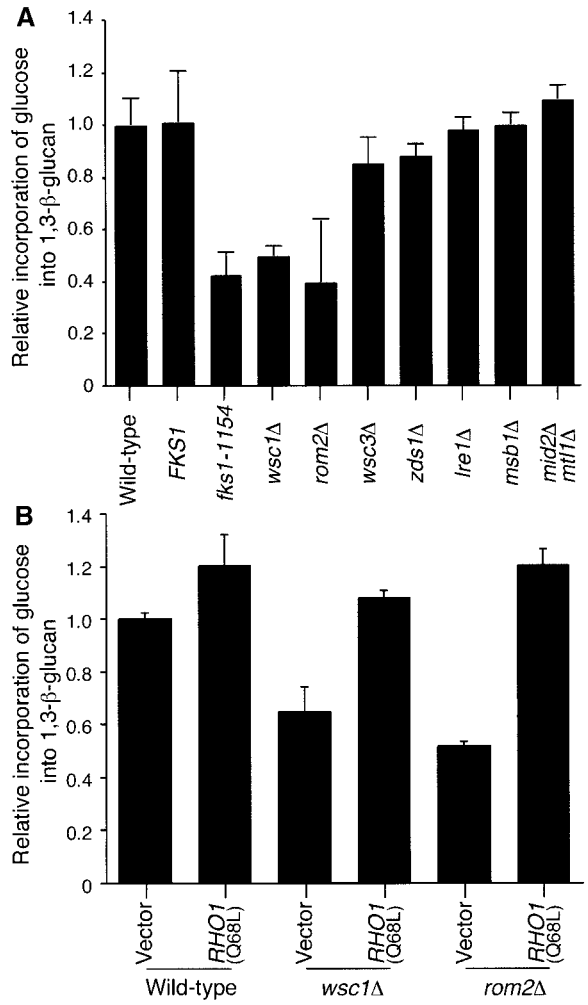

FIGURE 6.—1,3-β-glucan levels in deletion strains of the multicopy suppressor genes. (A) Cells were cultured to the log phase in YPD at 30° and incorporation of glucose into 1,3-β-glucan was measured. Strains used: YPH500 (wild type), YOC1001 (*FKS1*), YOC1087 (*fks1-1154*), YOC2573 (*wsc1*Δ), YOC2576 (*rom2*Δ), YOC2521 (*wsc3*Δ), YOC2581 (*zds1*Δ), YOC2579 (*lre1*Δ), YOC748 (*msb1*Δ), and YOC2526 (*mid2*Δ *mtl1*Δ). The data represent the means and standard deviations of at least three experiments. (B) Rescue of glucan synthesis of *wsc1*Δ and *rom2*Δ by the active form of *RHO1*. YPH500 (wild type), YOC2573 (*wsc1*Δ), or YOC2576 (*rom2*Δ) was transformed with the active form of *RHO1*. Cells were cultured in SD-Ura at 30° and incorporation of glucose into 1,3-β-glucan was measured. The means and standard deviations of at least three experiments are presented.

simply due to a loss of Fks1p localization. The partial loss of Fks1p localization in *wsc1*Δ and *rom2*Δ cells might be interpreted as a secondary effect of a defective cell wall structure, as was explained above with *fks1-1154* (Figure 1D). Together with these results, deletion analysis suggested that Wsc1p and Rom2p play a crucial role in glucan synthesis. Consistently, we observed a synthetic growth defect between *fks1-1154* and *wsc1*Δ, *rom2*Δ. To confirm that Rom2p and Wsc1p act as upstream regulators of GS through the activation of Rho1p, we tested suppression of the defects in growth and glucan synthesis of *wsc1*Δ and *rom2*Δ cells with a single copy of the activated form of Rho1p. The temperature-sensitive growth defect of *wsc1*Δ and *rom2*Δ cells at 37° (OZAKI *et al.* 1996; VERNA *et al.* 1997) was suppressed by expressing the active form

TABLE 5

1,3-β-Glucan levels in *rho1-2* cells with multiple copies of *MID2*, *WSC1*, and *ROM2* at 34°

Strain (plasmid)	Relative incorporation into 1,3-β-glucan
rho1-2 (pYO326)	1.00 ± 0.02
rho1-2 (YEpU-*MID2*)	1.05 ± 0.01
rho1-2 (YEpU-*WSC1*)	1.43 ± 0.21
rho1-2 (YEpU-*ROM2*)	1.85 ± 0.38
RHO1 (pYO326)	2.74 ± 0.22

The means and standard deviations of at least three experiments are presented.

of Rho1p. Moreover, glucan synthesis was restored to the wild-type level by expressing the activated form of Rho1p (Figure 6B). Fluorescent measurements using aniline blue confirmed that expressing the activated form of Rho1p rescued the decrease in 1,3-β-glucan content in *wsc1*Δ and *rom2*Δ cells. These results suggest that Rom2p and Wsc1p activate GS at point(s) upstream of Rho1p.

A temperature-sensitive *rho1* mutant is suppressed by the multicopy suppressors of *fks1-1154*: We examined genetic interactions between the multicopy suppressors and the regulatory subunit of GS. Temperature-sensitive *rho1-2* mutant cells were employed in this experiment because they showed both decreased *in vitro* GS activity (Qadota *et al.* 1996) and decreased incorporation of labeled glucose into 1,3-β-glucan (Table 5). We found that all of the multicopy suppressors (*WSC1*, *WSC3*, *MTL1*, *ROM2*, *LRE1*, *ZDS1*, and *MSB1*) effectively suppressed the temperature-sensitive growth defect of the *rho1-2* mutant (Figure 7A) and that the suppression was detectable even at 37°. The interpretation of this genetic data, however, is complex, since Rho1p is a multifunctional protein that affects five downstream effector proteins. Mutations of Rho1p result in actin delocalization (Helliwell *et al.* 1998) and cell lysis phenotypes (Kamada *et al.* 1996), both of which are characteristic phenotypes caused by the defect of the Pkc1p-MAPK cascade. These results indicate that the *rho1-2* mutation most likely impairs both 1,3-β-glucan synthesis and the Pkc1p-MAPK cascade. Therefore, although overexpression of *WSC1* and *ROM2* indeed increased the incorporation level of glucose into 1,3-β-glucan in *rho1-2* cells (Table 5) and the amount of 1,3-β-glucan, the possibility that the growth suppression of the *rho1-2* mutation by *WSC1* and *ROM2* was achieved by activation of the Pkc1p-MAPK cascade cannot be excluded.

MID2 effectively suppressed the temperature-sensitive growth defect of the *rho1-2* mutant (Figure 7A). Measurement of the incorporation revealed that overexpression of *MID2* did not increase the amount of 1,3-β-glucan in *rho1-2* cells (Table 5). In addition, several genetic studies revealed that *MID2* is placed upstream of the Pkc1p-MAPK cascade and Rho1p (Ketela *et al.* 1999; Rajavel *et al.* 1999; Andrews and Stark 2000; Marcoux *et al.* 2000; Philip and Levin 2001). Therefore, the most probable explanation is that the growth suppression of the *rho1-2* mutant by *MID2* is through activation of the Pkc1p-MAPK cascade.

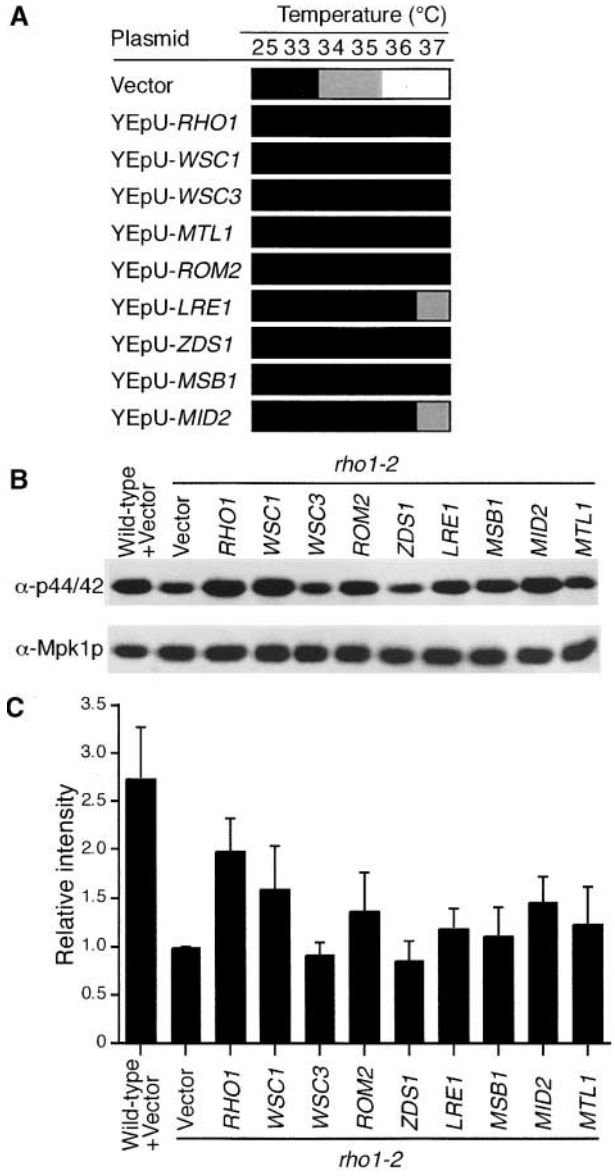

Figure 7.—Interactions between the suppressors and the Pkc1p-MAPK cascade regulated by Rho1p. (A) Growth of *rho1-2* cells transformed with one of the multicopy suppressors. YOC752 (*rho1-2*) was transformed with a 2μ plasmid (YEpU-*RHO1*, YEpU-*WSC1*, YEpU-*WSC3*, YEpU-*MTL1*, YEpU-*ROM2*, YEpU-*LRE1*, YEpU-*ZDS1*, YEpU-*MSB1*, or YEpU-*MID2*). At the six indicated temperatures growth of the transformants on YPD plates was scored. The results are presented as in Figure 2B. (B) Mpk1p phosphorylation in *rho1-2* transformed with one of the suppressors. The transformants in A were shifted to 39° for 2 hr and then blotted with either an anti-phospho-p44/42 MAPK antibody or an anti-MAPK antibody. (C) Quantification of Mpk1p phosphorylation. The amount of Mpk1p phosphorylation was quantified with LAS-1000plus (Fuji Photo Film). The means and standard deviations of at least three experiments are presented.

Pkc1p-MAPK cascade is activated by overexpression of *WSC1*, *ROM2*, *LRE1*, *MSB1*, *MTL1*, and *MID2*: We directly examined whether the suppressors act upstream of the Pkc1p-MAPK cascade by monitoring the phosphorylation state of Mpk1p with a specific antibody upon heat shock in *rho1-2* mutant cells transformed with suppressors. As shown in Figure 7B, we found that overexpression of *WSC1*, *ROM2*, and *MID2* significantly rescued the defect of Mpk1p phosphorylation upon heat shock (39°) in *rho1-2* cells. Quantitative analysis revealed that overexpression of *LRE1*, *MSB1*, and *MTL1* also rescued the reduced level but the effect was relatively minor (Figure 7C). Overexpression of *WSC3* and *ZDS1* showed little effect on Mpk1p phosphorylation. To rule out the possibility that the 39° heat shock is too severe for *rho1-2* mutant cells, we also monitored Mpk1p phosphorylation at a moderately high temperature (37°). At 37°, Mpk1p was slightly less phosphorylated in wild-type cells and overexpression of *WSC3* and *ZDS1* showed little effect on the degree of phosphorylation. These results suggest that among the multicopy suppressors, *WSC1*, *ROM2*, *LRE1*, *MSB1*, *MTL1*, and *MID2* act positively on the Pkc1p-MAPK cascade. On the basis of these results and those shown in Figure 3 and Table 3, we conclude that *WSC1*, *ROM2*, *LRE1*, *MSB1*, and *MTL1* positively regulate both 1,3-β-glucan synthesis and the Pkc1p-MAPK cascade, while *MID2* is involved mainly in the Pkc1p-MAPK cascade. *ZDS1* mainly regulates 1,3-β-glucan synthesis. *WSC3* mainly regulates 1,3-β-glucan synthesis but we could not rule out the possibility that *WSC3* has a minor effect on both effectors.

DISCUSSION

Identification of upstream regulators of Fks1p: Although the main components of GS, Fks1p and Rho1p, play crucial roles in defining cell shape during the budding cycle, no regulatory factors other than Rho1p have yet been suggested. Using aniline blue and glucose incorporation, we monitored cell wall glucan synthesis and showed that Wsc1p, Wsc3p, Mtl1p, Rom2p, Lre1p, Zds1p, and Msb1p act positively on glucan synthesis. We also present the first *in vivo* evidence suggesting that the active form of Rho1p promotes glucan synthesis.

All the suppressor genes isolated act positively on 1,3-β-glucan synthesis. Under the vegetative growth condition, these suppressors seem to act through Fks1p/Fks2p, but not other GS, since the suppressors did not suppress the synthetic lethality of *fks1*Δ *fks2*Δ double mutants. This is consistent with the observation that Fks3p, possibly another subunit of GS, is not expressed under the vegetative growth condition (our unpublished results). We did not isolate the factors involved in the synthesis of other cell wall components (*e.g.*, mannan, chitin, and 1,6-β-glucan). Recently, a mutation in *FKS1* was reported to show a synthetic growth defect with *chs3*, which is involved in chitin synthesis (Osmond *et al.* 1999), implying that different cell wall components act cooperatively on cell wall structure. However, our data suggest that any compensation of other cell wall materials does not suppress the defect of the 1,3-β-glucan biogenesis pathway.

GS activities of the *fks1-1154* mutant at the restrictive temperature are reduced more severely than those at the permissive temperature *in vivo* and *in vitro*. However, the difference in the GS activity between the permissive temperature and the restrictive temperature is small while the viability of *fks1-1154* cells is decreased severely at the restrictive temperature. We suppose that a threshold of the required minimum value for viability between the small differences in the activity of Fks1-1154p may exist. Introduction of multicopy suppressors increased 1,3-β-glucan in *fks1-1154* cells, but the effect on GS activity was small. Possibly a small increase in GS activity by overexpressing multicopy suppressors crosses over the minimum value for viability and the multicopy suppressors effectively suppress growth defects in *fks1-1154* cells.

Possible functions of the multicopy suppressors: Of the multicopy suppressors of the *fks1-1154* mutation, several are putative upstream regulators of Rho1p and Pkc1p, including Rom2p, which is a GEF of Rho1p (Ozaki *et al.* 1996). Wsc family proteins (including Wsc1p, Wsc2p, Wsc3p, and Wsc4p) and the Mid2p homolog, Mtl1p, are putative cell wall surface sensors essential for cell integrity signaling (Gray *et al.* 1997; Verna *et al.* 1997; Jacoby *et al.* 1998; Rajavel *et al.* 1999; Ketela *et al.* 1999; Philip and Levin 2001). Although the Pkc1p-MAPK cascade is involved in transcription of cell wall biogenesis genes, including *FKS1* (Igual *et al.* 1996; Jung and Levin 1999), activation of the Pkc1p-MAPK cascade by overexpressing Pkc1p or Mid2p in *fks1-1154* had little effect on the activation of GS (see results). Furthermore, we found that overexpression of the other two Rho1p targets, *BNI1* and *SKN7*, had little effect on growth of *fks1-1154* cells (our unpublished results). Together with these results, we propose that activation of 1,3-β-glucan synthesis occurs through direct activation of GS by Rho1p and that Fks1p and Pkc1p are activated independently by distinct upstream regulators. This idea is further supported by evidence that Mpk1p phosphorylation is defective in *mid2*Δ cells (Ketela *et al.* 1999; Rajavel *et al.* 1999) while *mid2*Δ cells have a normal content of 1,3-β-glucan (see results).

How do Wsc family proteins and Rom2p regulate glucan synthesis? It has been suggested that Wsc1p and Rom2p interact with each other (Philip and Levin 2001) and that these factors are important for activation of the Pkc1p-MAPK cascade upon environmental stress (Gray *et al.* 1997; Verna *et al.* 1997; Martín *et al.* 2000) and for relocalization of Fks1p upon heat shock (Delley and Hall 1999). However, no evidence indicates that Wsc1p and Rom2p are required for activation of 1,3-β-glucan synthesis. Here we show that *wsc1*Δ and *rom2*Δ cells exhibit a significant defect in 1,3-β-glucan synthesis

even at the permissive temperature (Figures 5A and 6). This is the first evidence suggesting that Wsc1p and Rom2p play roles in 1,3-β-glucan synthesis as well as in the Pkc1p-MAPK cascade during normal budding. As reported previously, Wsc1p localization is dependent on the polarized actin cytoskeleton (Delley and Hall 1999). Although more detailed analysis concerning the timing of Wsc1p localization is needed, it is conceivable that localization of Wsc1p might depend on polarization of the actin cytoskeleton achieved by Cdc42p.

Although Lre1p, Zds1p, and Msb1p were not known to be involved in cell wall synthesis, we found that *LRE1*, *ZDS1*, and *MSB1* act positively on 1,3-β-glucan synthesis (Figure 3 and Table 3). Of all the multicopy suppressors of the *fks1-1154* mutation identified, only *MSB1* showed a significant increase of *in vitro* glucan synthesis (Figure 4), suggesting that Msb1p does not act on the GDP-to-GTP exchange on Rho1p. At least two possibilities are consistent with this result. One possibility is that Msb1p is a component of the GS complex. However, Msb1p was apparently lost during preparation of the purified GS fraction, suggesting that Msb1p is not a tightly bound component of the GS complex. The other possibility is that Msb1p increases the GS complex. In fact, the amounts of Fks1p and Rho1p were slightly increased by expression of Msb1p in *fks1-1154* or *rho1-2* cells (our unpublished results). This result suggests that *MSB1* acts on GS positively by increasing the expression of GS components or by stabilizing the GS complex. Since *msb1*Δ cells did not exhibit a clear effect on GS activity, there may be a factor(s) that has a redundant function of Msb1p. It should be noted that *MSB1* suppresses a mutation in *BEM4*, which encodes a protein that physically interacts with multiple types of Rho-type GTPase without affecting their GDP-GTP exchange cycle (Mack *et al.* 1996). Msb1p might function through a mechanism shared with Bem4p. Lre1p and Zds1p are novel components related to Rho1p. Although more study will be necessary to know the precise molecular mechanism of their functions, we will discuss their involvement in Rho1p-regulated pathways below.

Relationship between the suppressors and Rho1p: We showed that all suppressor genes examined are genetically related to Rho1p and summarize the results of their effects on the Pkc1p-MAPK cascade and GS in Figure 8. The suppressors were classified into three groups: *WSC1*, *ROM2*, *LRE1*, *MSB1*, and *MTL1* regulate both 1,3-β-glucan synthesis and the Pkc1p-MAPK pathway, and *ZDS1* mainly regulates 1,3-β-glucan synthesis, while *MID2* mainly regulates the Pkc1p-MAPK pathway. *WSC3* regulates 1,3-β-glucan synthesis or both effectors of Rho1p. Thus, we show that the two essential Rho1p targets, Fks1p and Pkc1p, have distinct upstream regulators. Moreover, among the positive factors of 1,3-β-glucan synthesis tested, *WSC1*, *WSC3*, *MTL1*, *ROM2*, *LRE1*, and *ZDS1* act through activation of Rho1p, while *MSB1* does not.

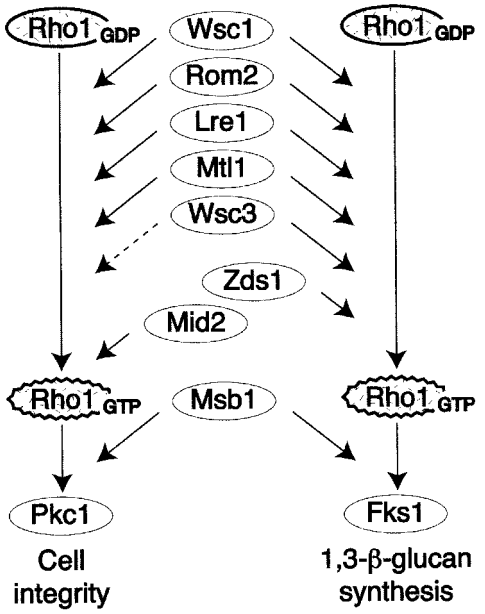

Figure 8.—Distinct effects of Rho1p-related components on activation of Fks1p and Pkc1p. We showed that different components genetically related to Rho1p (Wsc1p, Wsc3p, Mid2p, Mtl1p, Rom2p, Msb1p, Lre1p, and Zds1p) affect the Rho1p effectors, Fks1p and Pkc1p, differently.

In this article, we proposed a model for the function of the suppressors under vegetative growth conditions. It is quite interesting to test the possibility that the subset of upstream components for the Rho1p targets could be different under different physiological conditions. For example, *MID2* is known to be important for sensing cell wall stress both during vegetative growth and pheromone-induced conditions (Ono *et al.* 1994; Ketela *et al.* 1999; Rajavel *et al.* 1999). Future study needs to address whether Mid2p has a different subset of downstream regulators under these conditions.

In mammalian cells, GTP-bound Ras triggers several cellular activities, including cell proliferation, malignant transformation, differentiation, and apoptosis, depending on different cell types (Satoh and Kaziro 1992; Campbell *et al.* 1998). Like Rho1p, Ras has various kinds of upstream regulators (receptor-tyrosine kinases) and downstream effectors. Although unproven in mammalian cells, it is assumed that various activities are caused by different combinations of effector molecules. In yeast, it is known that *RHO1* may activate a subset of effectors during cytoskeletal organization (Helliwell *et al.* 1998). However, no explanation has yet been offered on how various pathways are regulated by small GTPases.

Here we demonstrated that putative upstream regulators of Rho1p have major effects on the different effectors, Fks1p and Pkc1p. What is the determinant of this different effect? It seems important that C-terminal amino acid sequences of Mid2p, which fall in the putative cytoplasmic domain, are different from the corresponding sequences of Mtl1p, Wsc1p, and Wsc3p. In

consideration of the previous report (Philip and Levin 2001), all these Wsc family proteins may interact with Rom2p and activate Rho1p, which is consistent with our results. Possibly each cytoplasmic domain of Wsc family proteins acts as a scaffold that assembles Rom2p and different Rho1p effector complexes. It is important to identify molecules interacting with the cytoplasmic domains and also necessary to know which signals reside in Mid2p, Mtl1p, Wsc1p, and Wsc3p. It has already been suggested that stress signals responsible for Pkc1p-MAPK activation are different in different Wsc-related proteins (Ketela *et al.* 1999; De Nobel *et al.* 2000; Martín *et al.* 2000) and that different Wsc-related proteins are modified by different factors (Philip and Levin 2001).

In conclusion, we identified putative regulatory components of 1,3-β-glucan synthesis using *fks1-1154*. We also suggested a network of regulatory components upstream of the two Rho1p effectors, Fks1p and Pkc1p. Future study will include determination of the functions of the regulators in cell cycle progression, screening of more mutants with defects in 1,3-β-glucan synthesis, and investigation of interactions of the regulatory components at the molecular level. Further investigation of the specificity of signals upstream of Rho1p effectors will give us a key to answering how orchestration of small GTPase protein functions can be achieved.

We thank Kana Morishita and Hiroshi Qadota for initiating this project. We also thank Kazuma Tanaka for providing us the *PKC1* (R398P) allele and David Levin for giving us the *BCK1-20* allele. We are also grateful to Keiichi Homma for critically reading the manuscript and members of the Laboratory of Signal Transduction for helpful discussion. This work was supported by grants from the Ministry of Education, Science, and Sports and Culture of Japan to Y. Ohya and from the Japan Society for the Promotion of Science for Young Scientists to M. Abe.

LITERATURE CITED

Abe, M., I. Nishida, M. Minemura, H. Qadota, S. Seyama *et al.*, 2001 Yeast 1,3-β-glucan synthase activity is inhibited by phytosphingosine localized to the endoplasmic reticulum. J. Biol. Chem. **276:** 26923–26930.

Alberts, A. S., N. Bouquin, L. H. Johnston and R. Treisman, 1998 Analysis of RhoA-binding proteins reveals an interaction domain conserved in heterotrimeric G protein β subunits and the yeast response regulator protein Skn7. J. Biol. Chem. **273:** 8616–8622.

Andrews, P. D., and M. J. Stark, 2000 Type 1 protein phosphatase is required for maintenance of cell wall integrity, morphogenesis and cell cycle progression in *Saccharomyces cerevisiae*. J. Cell Sci. **113:** 507–520.

Bender, A., and J. R. Pringle, 1989 Multicopy suppression of the *cdc24* budding defect in yeast by *CDC42* and three newly identified genes including the ras-related gene *RSR1*. Proc. Natl. Acad. Sci. USA **86:** 9976–9980.

Bi, E., and J. Pringle, 1996 *ZDS1* and *ZDS2*, genes whose products may regulate Cdc42p in *Saccharomyces cerevisiae*. Mol. Cell. Biol. **16:** 5264–5275.

Bickle, M., P. A. Delley, A. Schmidt and M. N. Hall, 1998 Cell wall integrity modulates *RHO1* activity via the exchange factor *ROM2*. EMBO J. **17:** 2235–2245.

Bouquin, N., A. L. Johnson, B. A. Morgan and L. H. Johnston, 1999 Association of the cell cycle transcription factor Mbp1 with the Skn7 response regulator in budding yeast. Mol. Biol. Cell **10:** 3389–3400.

Brown, J. L., H. Bussey and R. C. Stewart, 1994 Yeast Skn7p functions in a eukaryotic two-component regulatory pathway. EMBO J. **13:** 5186–5194.

Cabib, E., J. Drgonová and T. Drgon, 1998 Role of small G proteins in yeast cell polarization and wall biosynthesis. Annu. Rev. Biochem. **67:** 307–333.

Campbell, S. L., R. Khosravi-Far, K. L. Rossman, G. J. Clark and C. J. Der, 1998 Increasing complexity of Ras signaling. Oncogene **17:** 1395–1413.

Cid, V. J., A. Durán, F. Del Rey, M. P. Snyder, C. Nombela *et al.*, 1995 Molecular basis of cell integrity and morphogenesis in *Saccharomyces cerevisiae*. Microbiol. Rev. **59:** 345–386.

Debono, M., and R. S. Gordee, 1994 Antibiotics that inhibit fungal cell wall development. Annu. Rev. Microbiol. **48:** 471–497.

Delley, P.-A., and M. N. Hall, 1999 Cell wall stress depolarizes cell growth *via* hyperactivation of *RHO1*. J. Cell Biol. **147:** 163–174.

De Nobel, H., C. Ruiz, H. Martin, W. Morris, S. Brul *et al.*, 2000 Cell wall perturbation in yeast results in dual phosphorylation of the Slt2/Mpk1 MAP kinase and in an Slt2-mediated increase in *FKS2–lacZ* expression, glucanase resistance and thermotolerance. Microbiology **146:** 2121–2132.

Douglas, C. M., F. Foor, J. A. Marrinan, N. Morin, J. B. Nielsen *et al.*, 1994 The *Saccharomyces cerevisiae FKS1* (*ETG1*) gene encodes an integral membrane protein which is a subunit of 1,3-β-D-glucan synthase. Proc. Natl. Acad. Sci. USA **91:** 12907–12911.

Drgonová, J., T. Drgon, K. Tanaka, R. Kollár, G.-C. Chen *et al.*, 1996 Rho1p, a yeast protein at the interface between cell polarization and morphogenesis. Science **272:** 277–279.

Evangelista, M., K. Blundell, M. S. Longtine, C. J. Chow, N. Adames *et al.*, 1997 Bni1p, a yeast formin linking Cdc42p and the actin cytoskeleton during polarized morphogenesis. Science **276:** 118–122.

Evans, N. A., and P. A. Hoyne, 1984 Characteristics and specificity of the interaction of fluorochrome from aniline blue (sirofluor) with polysaccharides. Carbohydr. Polymers **4:** 215–230.

Gray, J. V., J. P. Ogas, Y. Kamada, M. Stone, D. E. Levin *et al.*, 1997 A role for the Pkc1 MAP kinase pathway of *Saccharomyces cerevisiae* in bud emergence and identification of a putative upstream regulator. EMBO J. **16:** 4924–4937.

Guo, W., F. Tamanoi and P. Novick, 2001 Spatial regulation of the exocyst complex by Rho1 GTPase. Nat. Cell Biol. **3:** 353–360.

Hector, R. F., 1993 Compounds active against cell walls of medically important fungi. Clin. Microbiol. Rev. **6:** 1–21.

Helliwell, S. B., A. Schmidt, Y. Ohya and M. N. Hall, 1998 The Rho1 effector Pkc1, but not Bni1, mediates signalling from Tor2 to the actin cytoskeleton. Curr. Biol. **8:** 1211–1214.

Hirano, H., K. Tanaka, K. Ozaki, H. Imamura, H. Kohno *et al.*, 1996 *ROM7/BEM4* encodes a novel protein that interacts with the Rho1p small GTP-binding protein in *Saccharomyces cerevisiae*. Mol. Cell. Biol. **16:** 4396–4403.

Ho, S. N., H. D. Hunt, R. M. Horton, J. K. Pullen and L. R. Pease, 1989 Site-directed mutagenesis by overlap extension using the polymerase chain reaction. Gene **77:** 51–59.

Hong, A., P. Mann, K. J. Shaw and B. Didomenico, 1994 Analysis of β-glucans and chitin in *Saccharomyces cerevisiae* cell wall mutant using high-performance liquid chromatography. Yeast **10:** 1083–1092.

Igual, J. C., A. L. Johnson and L. H. Johnston, 1996 Coordinated regulation of gene expression by the cell cycle transcription factor Swi4 and the protein kinase C MAP kinase pathway for yeast cell integrity. EMBO J. **15:** 5001–5013.

Imamura, H., K. Tanaka, T. Hihara, M. Umikawa, T. Kamei *et al.*, 1997 Bni1p and Bnr1p: downstream targets of the Rho1 family small G-proteins which interact with profilin and regulate actin cytoskeleton in *Saccharomyces cerevisiae*. EMBO J. **16:** 2745–2755.

Inoue, S. B., N. Takewaki, T. Takasuka, T. Mio, M. Adachi *et al.*, 1995 Characterization and gene cloning of 1,3-β-D-glucan synthase subunit from *Saccharomyces cerevisiae*. Eur. J. Biochem. **231:** 845–854.

Ito, H., Y. Fukuda, K. Murata and A. Kimura, 1983 Transformation of intact yeast cells treated with alkali cations. J. Bacteriol. **153:** 163–168.

Jacoby, J. J., S. M. Nilius and J. J. Heinisch, 1998 A screen for upstream components of the yeast protein kinase C signal trans-

duction pathway identifies the product of the *SLG1* gene. Mol. Gen. Genet. **258:** 148–155.

Jones, J. S., and L. Prakash, 1990 Yeast *Saccharomyces cerevisiae* selectable markers in pUC18 polylinkers. Yeast **6:** 363–366.

Jung, U. J., and D. Levin, 1999 Genome-wide analysis of gene expression regulated by the yeast cell wall integrity signalling pathway. Mol. Microbiol. **34:** 1049–1057.

Kaiser, C. A., S. Michaelis and A. Mitchell, 1994 *Methods in Yeast Genetics: A Laboratory Course Manual*. Cold Spring Harbor Laboratory Press, Cold Spring Harbor, NY.

Kamada, Y., U. S. Jung, J. Piotrowski and D. E. Levin, 1995 The protein kinase C-activated MAP kinase pathway of *Saccharomyces cerevisiae* heat shock response. Genes Dev. **9:** 1559–1571.

Kamada, Y., H. Qadota, C. P. Python, Y. Anraku, Y. Ohya *et al.*, 1996 Activation of yeast protein kinase C by Rho1 GTPase. J. Biol. Chem. **271:** 9193–9196.

Kelly, R., E. Register, M. J. Hsu, M. Kurtz and J. Nielsen, 1996 Isolation of a gene involved in 1,3-β-glucan synthesis in *Aspergillus nidulan*s and purification of the corresponding protein. J. Bacteriol. **178:** 4381–4391.

Ketela, T., R. Green and H. Bussey, 1999 *Saccharomyces cerevisiae* Mid2p is a potential cell wall stress sensor and upstream activator of the PKC1-MPK1 cell integrity pathway. J. Bacteriol. **181:** 3330–3340.

Kohno, H., K. Tanaka, A. Mino, M. Umikawa, H. Imamura *et al.*, 1996 Bni1p implicated in cytoskeletal control is a putative target of Rho1p small GTP binding protein in *Saccharomyces cerevisiae*. EMBO J. **15:** 6060–6068.

Lai, M. H., S. J. Silverman, J. P. Gaughran and D. R. Kirsch, 1997 Multiple copies of *PBS2*, *MHP1* or *LRE1* produce glucanase resistance and other cell wall effects in *Saccharomyces cerevisiae*. Yeast **13:** 199–213.

Lee, K. G., and D. E. Levin, 1992 Dominant mutations in a gene encoding a putative protein kinase (*BCK1*) bypass the requirement for a *Saccharomyces cerevisiae* protein kinase C homolog. Mol. Cell. Biol. **12:** 172–182.

Lodder, A. L., T. K. Lee and R. Ballester, 1999 Characterization of the Wsc1 protein, a putative receptor in the stress response of *Saccharomyces cerevisiae*. Genetics **152:** 1487–1499.

Mack, D., K. Nishimura, B. K. Dennehey, T. Arbogast, J. Parkinson *et al.*, 1996 Identification of the bud emergence gene *BEM4* and its interactions with rho-type GTPases in *Saccharomyces cerevisiae*. Mol. Cell. Biol. **16:** 4387–4395.

Marcoux, N., S. Cloutier, E. Zakrzewska, P.-M. Charest, Y. Bourbonnais *et al.*, 2000 Suppression of the profilin-deficient phenotype by the RHO2 signaling pathway in *Saccharomyces cerevisiae*. Genetics **156:** 579–592.

Martín, H., J. M. Rodríguez-Pachón, C. Ruiz, C. Nombela and M. Molina, 2000 Regulatory mechanisms for modulation of signaling through the cell integrity Slt2-mediated pathway in *Saccharomyces cerevisiae*. J. Biol. Chem. **275:** 1511–1519.

Mazur, P., and W. Baginsky, 1996 *In vitro* activity of 1,3-β-D-glucan synthase requires the GTP-binding protein Rho1. J. Biol. Chem. **271:** 14604–14609.

Mazur, P., N. Morin, W. Baginsky, M. El-Sherbeini, J. A. Clemas *et al.*, 1995 Differential expression and function of two homologous subunits of yeast 1,3-β-glucan synthase. Mol. Cell. Biol. **15:** 5671–5681.

Morgan, B. A., G. R. Banks, W. M. Toone, D. Raitt, S. Kuge *et al.*, 1997 The Skn7 response regulator controls gene expression in the oxidative stress response of the budding yeast *Saccharomyces cerevisiae*. EMBO J. **16:** 1035–1044.

Nonaka, H., K. Tanaka, H. Hirano, T. Fujiwara, H. Kohno *et al.*, 1995 A downstream target of *RHO1* small GTP-binding protein is *PKC1*, a homolog of protein kinase C, which leads to activation of the MAP kinase cascade in *Saccharomyces cerevisiae*. EMBO J. **14:** 5931–5938.

Ono, T., T. Suzuki, Y. Anraku and H. Iida, 1994 The *MID2* gene encodes a putative integral membrane protein with a Ca^{2+}-binding domain and shows mating pheromone-stimulated expression in *Saccharomyces cerevisiae*. Gene **151:** 203–208.

Osmond, B. C., C. A. Specht and P. W. Robbins, 1999 Chitin synthase III: synthetic lethal mutants and "stress related" chitin synthesis that bypasses the *CSD3/CHS6* localization pathway. Proc. Natl. Acad. Sci. USA **96:** 11206–11210.

Ozaki, K., K. Tanaka, H. Imamura, T. Hihara, T. Kameyama *et al.*, 1996 Rom1p and Rom2p are GDP/GTP exchange proteins (GEPs) for the Rho1p small GTP binding protein in *Saccharomyces cerevisiae*. EMBO J. **15:** 2196–2207.

Paravicini, G., M. Cooper, L. Friedli, D. J. Smith, J.-L. Carpentier *et al.*, 1992 The osmotic integrity of the yeast cell requires a functional *PKC1* gene product. Mol. Cell. Biol. **12:** 4896–4905.

Philip, B., and D. E. Levin, 2001 Wsc1 and Mid2 are cell surface sensors for cell wall integrity signaling that act through Rom2, a guanine nucleotide exchange factor for Rho1. Mol. Cell. Biol. **21:** 271–280.

Pringle, J. R., R. A. Peterson, A. E. M. Adams, T. Sterns, D. G. Drubin *et al.*, 1989 Fluorescence microscopy methods in yeast. Methods Cell Biol. **31:** 357–436.

Pruyne, D., and A. Bretscher, 2000a Polarization of cell growth in yeast. I. Establishment and maintenance of polarity states. J. Cell Sci. **113:** 365–375.

Pruyne, D., and A. Bretscher, 2000b Polarization of cell growth in yeast. II. The role of the cortical actin organization. J. Cell Sci. **113:** 571–585.

Qadota, H., Y. Anraku, D. Botstein and Y. Ohya, 1994 Conditional lethality of yeast strain expressing human *RHOA* in place of *RHO1*. Proc. Natl. Acad. Sci. USA **91:** 9317–9321.

Qadota, H., C. P. Python, S. B. Inoue, M. Arisawa, Y. Anraku *et al.*, 1996 Identification of yeast Rho1p GTPase as a regulatory subunit of 1,3-β-glucan synthase. Science **272:** 279–281.

Rajavel, M., B. Philip, B. M. Buehrer, B. Errede and D. E. Levin, 1999 Mid2 is a putative sensor for cell integrity signaling in *Saccharomyces cerevisiae*. Mol. Cell. Biol. **19:** 3969–3976.

Ram, A. F., A. Wolters, R. ten Hoopen and F. M. Klis, 1994 A new approach for isolating cell wall mutants in *Saccharomyces cerevisiae* by screening for hypersensitivity to Calcofluor white. Yeast **10:** 1019–1030.

Roncero, C., and A. Durán, 1985 Effect of Calcofluor white and Congo red on fungal cell wall morphogenesis: in vivo activation of chitin polymerization. J. Bacteriol. **163:** 1180–1185.

Roy, N., and K. W. Runge, 1999 The *ZDS1* and *ZDS2* proteins require the Sir3p component of yeast silent chromatin to enhance the stability of short linear centromeric plasmids. Chromosoma **108:** 146–161.

Sakumoto, N., Y. Mukai, K. Uchida, T. Kouchi, J. Kuwajima *et al.*, 1999 A series of protein phosphatase gene disruptants in *Saccharomyces cerevisiae*. Yeast **15:** 1669–1679.

Sambrook, J., E. F. Fritsch and T. Maniatis, 1989 *Molecular Cloning: A Laboratory Manual*. Cold Spring Harbor Laboratory Press, Cold Spring Harbor, NY.

Satoh, T., and Y. Kaziro, 1992 Ras insignal transduction. Semin. Cancer Biol. **3:** 169–177.

Shedletzky, E., C. Unger and D. P. Delmer, 1997 A microtiter-based fluorescence assay for (1,3)-β-glucan synthases. Anal. Biochem. **249:** 88–93.

Sikorski, R. S., and P. Hieter, 1989 A system of shuttle vectors and yeast host strains designed for efficient manipulation of DNA in *Saccharomyces cerevisiae*. Genetics **122:** 19–27.

Verna, J., A. Lodder, K. Lee, A. Vagts and R. Ballester, 1997 A family of genes required for maintenance of cell wall integrity and for the stress response in *Saccharomyces cerevisiae*. Proc. Natl. Acad. Sci. USA **94:** 13804–13809.

Watanabe, D., M. Abe and Y. Ohya, 2001 Yeast Lrg1p acts as a specialized RhoGAP regulating 1,3-β-glucan synthesis. Yeast **18:** 943–951.

Yoshihisa, T., and Y. Anraku, 1989 Nucleotide sequence of *AMS1*, the structural gene of vacuolar α-mannosidase of *Saccharomyces cerevisiae*. Biochem. Biophys. Res. Commun. **163:** 908–915.

Yu, Y., Y. W. Jiang, R. J. Wellinger, K. Carlson, J. M. Roberts *et al.*, 1996 Mutations in the homologous *ZDS1* and *ZDS2* genes affect cell cycle progression. Mol. Cell. Biol. **16:** 5254–5263.

Communicating editor: M. D. Rose